

Bandlimited Field Reconstruction from Samples Obtained at Unknown Random Locations on a Grid

Ankur Mallick and Animesh Kumar
Department of Electrical Engineering
Indian Institute of Technology Bombay
Mumbai, India 400076

Email: ankur.mallick24@gmail.com, animesh@ee.iitb.ac.in

Abstract—We study the sampling of spatial fields using sensors that are location-unaware but deployed according to a known statistical distribution. It has been shown that uniformly distributed location-unaware sensors cannot infer bandlimited fields due to the symmetry and shift-invariance of the field.

This work studies asymmetric (nonuniform) distributions on location-unaware sensors that will enable bandlimited field inference. For the sake of analytical tractability, location-unaware sensors are restricted to a *discrete grid*. Oversampling followed by clustering of the samples using the probability distribution that governs sensor placement on the grid is used to infer the field. Based on this clustering algorithm, the main result of this work is to find the *optimal* probability distribution on sensor locations that minimizes the detection error-probability of the underlying spatial field. The proposed clustering algorithm is also extended to include the case of signal reconstruction in the presence of sensor noise by treating the distribution of the noisy samples as a mixture model and using clustering to estimate the mixture model parameters.

I. INTRODUCTION

Distributed sensing of spatial fields using an array of distributed low-power sensors is an active area of interest. In the past, sampling techniques have been proposed as one method of distributed sensing, where the spatial field can be modeled as a distributed signal [1], [2], [3], [4], [5], [6], [7]. In all these works and many more, a central theme is that the location of sensors is known. In practice, the location of sensor can be ascertained by localization algorithms [8], [9], or by using extra equipment such as a GPS receiver (global positioning system receiver). These techniques will have added cost in terms of power used and hardware required. An alternate option to having expensive sensors or expensive localization algorithms is to work with sensors which are location unaware.

Recently, bandlimited field estimation with location unaware sensors in a distributed setup has been studied [10], [11]. This is an interesting paradigm where the key idea is to utilize a multitude of location unaware sensors (oversampling) and leverage the random distribution on their spatial locations to reconstruct the spatial field. In a negative result, it is known that uniformly distributed location unaware sensors do not infer the field uniquely up to a shift and a flip of the underlying signal [10]. The negative result has its root in the symmetry of a uniform distribution and the shift-invariance properties of bandlimited fields. In this work, it will be further noted that the negative result extends to the spatially scaled

versions of a bandlimited field as well. For example, spatial fields $g(x)$ and $g(2x)$ will be indistinguishable by readings observed from uniformly distributed location unaware sensors. These negative results motivate the study of an asymmetric (statistical) distribution of location unaware sensors, that may enable bandlimited field reconstruction.

A bandlimited field is a nonlinear function of the location. If the location of each sensor is random and unknown, then a bandlimited field operating on this randomness is observed through samples. This process is nonlinear and leads to difficult inference problems. To facilitate analysis, in this first exposition on the topic, the location of the sensors is restricted to a random point on an *equi-spaced discrete grid*.¹ The location unawareness of sensors will be overcome by using oversampling in our setup. For field reconstruction purposes, a technique is required which associates the samples of the field to their respective locations on the equi-spaced deterministic grid in the sampling interval of interest. One such technique is sample clustering as explained next.

With oversampling, samples obtained from sensors can be clustered together to infer which sample belongs to which spatial location on the equi-spaced grid where the sensors are present. The key insight behind our clustering method is as follows. All the sensors present at a location will record the same field value. The probability with which a sensor falls at any location in the deterministic grid is a parameter of choice. If p is the probability with which a sensor falls at a given location, then $\approx np$ will be the number of samples obtained from there, as n (total number of samples across all locations) becomes large. If the sensors have unequal probability of falling at different locations, the locations of samples can be *detected* by using their expected frequency. The success of this clustering scheme will depend on the probability distribution that governs sensor placement on the grid. One of the *main results* of this work is to find the *optimal* probability distribution on sensor locations that minimizes the detection error-probability of the underlying spatial field (see Section III).

Since samples obtained from real world signals are typically affected by measurement noise, the effect of additive noise on samples is also explored on our clustering algorithm and as-

¹This may arise in scenarios where location information is masked to preserve the identity of the sensors, or to reduce the amount of data that needs to be transmitted.

sociated field reconstruction. A different clustering approach, that banks upon methods used in machine learning, is used to associate the various field samples with their respective locations. Then, the observed noise-affected field samples are used to estimate the field values. The distribution of the noise-affected samples is modeled by a mixture model and the special case of Gaussian noise is analysed to show that our approach works fairly well in most cases even in the presence of noise. Simulation results are presented to verify our algorithm (see Section IV).

Prior art: Estimation of bandlimited fields from samples taken at unknown but statistically distributed sampling locations was studied by Kumar [10], [11]. Reconstruction of discrete-time bandlimited fields from unknown sampling locations was studied by Marziliano and Vetterli [12] in a combinatorial setting. Estimation of periodic bandlimited signals with random sampling locations has been studied by Nordio et al. [13], where the locations are obtained by a perturbation of the deterministic equi-spaced grid. Their work is related to estimation or “denoising” of bandlimited fields. In this work, sampling of physical fields is addressed via oversampling when sensor locations are restricted to a deterministic equi-spaced grid. Sensors are location unaware, and a clustering algorithm will be used to associate field samples with their respective locations. The design of probability distribution on sensor locations is addressed in this work to minimize the probability of incorrect association of field samples with the sampling locations on the equi-spaced grid. Finally, a clustering algorithm is presented in this work to tackle measurement noise at the sensors.

Notation: Space will be denoted by x . Spatial fields will be denoted by $g(x)$ and its variants, and the Fourier series coefficients will be denoted by $a[k]$ and its variants. Probability distribution function (pdf) of a random variable Y will be denoted by $f_Y(y)$. A Gaussian distribution with mean μ and standard deviation σ^2 will be denoted by $\mathcal{N}(\mu, \sigma^2)$, while $j = \sqrt{-1}$ will be the imaginary root of -1 . The probability and expectation operators will be denoted by \mathbb{P} and \mathbb{E} respectively. All vectors are column-vectors.

Organization: The sampling system model and the reconstruction methodology are presented in Section II. In Section III, the minimization of field detection error-probability is addressed. Throughout the analysis in this section it is assumed that the samples are not corrupted by any noise. In Section IV, the algorithm for field estimation from measurement-noise affected samples is addressed. Finally, conclusions are presented in Section V.

II. SYSTEM MODEL, RECONSTRUCTION, AND RELATED RESULTS

The spatial field model and its properties, the sampling model used, and related theoretical results are reviewed in this section in this section. The field model appears first.

A. Spatial field model

The spatial field varies with space and time. A distributed array of sensors will be used to acquire the field, so the

following model on the field will be applicable to each time snapshot of the field. Time snapshots of spatially one dimensional fields are considered. The spatial field $g(x)$ is assumed to be real valued, bounded, and have a finite spatial support in $[0, 1]$. It is assumed that the field has a Fourier series with finite number of terms, that is,

$$g(x) = \sum_{k=-b}^b a[k] \exp(j2\pi kx) \quad (1)$$

where $0 \leq x \leq 1$, and where $a[k]$ are the Fourier series coefficients of $g(x)$ and b is a *known* bandwidth parameter.

For simplicity of notation, define $s_b := 1/(2b+1)$ as a grid spacing parameter and $\phi_k := \exp(j2\pi k s_b)$, $-b \leq k \leq b$. Let Φ_b be defined as

$$\Phi_b = \begin{bmatrix} 1 & \dots & 1 \\ \phi_{-b} & \dots & \phi_b \\ \vdots & & \vdots \\ (\phi_{-b})^{2b} & \dots & (\phi_b)^{2b} \end{bmatrix}.$$

The columns of Φ_b are orthogonal and a sampling theorem ensures that [13], [14]:

$$\vec{a} = (\Phi_b)^{-1} \vec{g} = \frac{1}{(2b+1)} \Phi_b^\dagger \vec{g}, \quad (2)$$

where $\vec{a} = (a[-b], a[-b+1], \dots, a[b])^T$, where Φ_b^\dagger is the conjugate transpose of Φ_b , and $\vec{g} = (g(0), g(s_b), \dots, g(2bs_b))^T$. From (2), \vec{a} and $g(x)$ can be obtained using the samples in \vec{g} .

It will also be assumed that $g(is_b)$ are *distinct* for different values of $0 \leq i \leq 2b$. This feature will be useful in associating samples with their locations. The unequal values of the field at grid locations can be justified if the corresponding Fourier series coefficients are linearly independent continuous random variables. Let \vec{a} be the realization of a linearly independent continuous random vector (as may be the case for Fourier coefficients of naturally occurring fields). If $g(ms_b) = g(ns_b)$, then

$$\sum_{k=-b}^b a[k] (\exp(j2\pi k m s_b) - \exp(j2\pi k n s_b)) = 0. \quad (3)$$

This condition will be never satisfied, since \vec{a} is a linearly independent continuous random vector, and therefore its linear combination is non-zero almost surely.

B. Sensor deployment model

A discrete-valued non-uniform distribution is considered for bandlimited field inference. It will be assumed that a sensor is at location X such that $X = is_b$ with probability p_i where $i = 0, 1, \dots, 2b$ and $\sum_{i=0}^{2b} p_i = 1$. Correspondingly,

$$g(X) = g(is_b) \text{ with probability } p_i, \quad i = 0, 1, \dots, 2b \quad (4)$$

since it is assumed that $g(0), g(s_b), \dots, g(2bs_b)$ are distinct. In our model (illustrated in Fig. 1), the sensor falls at is_b , $0 \leq i \leq 2b$ but its location, that is the index i , is *not known*. The parameter $\vec{p} := p_0, p_1, \dots, p_{2b}$ will be treated as a *design choice* to optimize a performance criterion of choice (see

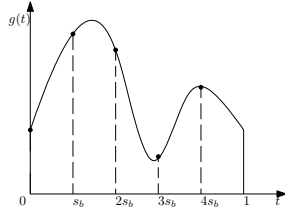


Fig. 1. Sampling model for a signal $g(t)$ with $b = 2$ i.e. $s_b = 1/5$.

Section III). It will be assumed that elements of \vec{p} are distinct (to break symmetry in the distribution of sensor-locations). Without loss of generality, it will be assumed that

$$p_0 < p_1 < \dots < p_{2b}. \quad (5)$$

In our sampling model, i.i.d. samples $g(X_1), g(X_2), \dots, g(X_n)$ are available for the detection of spatial field, where n corresponds to oversampling.²

C. Difficulty in field reconstruction with samples at uniformly distributed locations

To motivate the use of an asymmetric distribution on the sampling locations, we first consider the case where the unknown sampling locations are realized according to a uniform distribution, that is, $X \sim \text{Uniform}[0, 1]$. Let U_1, U_2, \dots, U_n be the (random) sampling locations according to this uniform distribution; then, the corresponding sampled field values are $g(U_1), g(U_2), \dots, g(U_n)$. For this section, also assume that $g(x)$ is bounded in amplitude. Without loss of generality, let $|g(x)| \leq 1$ for all $x \in [0, 1]$. The empirical cumulative distribution function

$$F_{g,n}(\theta) = \frac{1}{n} \sum_{i=1}^n \mathbb{1}(g(U_i) \leq \theta) \quad (6)$$

for $\theta \in [-1, 1]$ completely characterizes the field values $g(U_1), g(U_2), \dots, g(U_n)$ (up to a permutation) and vice-versa. By the Glivenko-Cantelli theorem, for every $\theta \in [-1, 1]$, $F_{g,n}(\theta)$ in (6) converges almost surely to $\mathbb{P}(g(U) \leq \theta)$. For a uniform random variable, $\mathbb{P}(g(U) \leq \theta)$ corresponds to length of the level set $\{u : g(u) \leq \theta\}$. It has been shown that a bandlimited field when shifted or space-reversed results in the same length of level set [10]. That is,

$$\mathbb{P}(g(U) \leq \theta) = \mathbb{P}(g_1(U) \leq \theta) = \mathbb{P}(g_2(U) \leq \theta) \quad (7)$$

where $g_1(t) = g(t - s)$ and $g_2(t) = g(s - t)$ for any $s \in [0, 1]$ and any $\theta \in [-1, 1]$. This means by observing the distribution $\mathbb{P}(g(U) \leq \theta)$, $\theta \in [-1, 1]$, the field $g(x)$ cannot be inferred due to ambiguity in phase and direction. However, it is not clear if shift and direction are the only ambiguities in the estimation of the field. In other words, is it possible to claim that the field can be obtained up to a delay and direction ambiguity as hinted in (7)? It is shown next that *scale ambiguity* is also

²It is desirable to address the setup where each sensor's location X is realized from an asymmetric continuous distribution supported in $[0, 1]$. In the limit of large number of measurements, the probability distribution of $g(X)$ random variable will be available. Since $g(x)$ is a non-linear function with oscillatory behavior, obtaining the Fourier series of $g(x)$ from the statistics of $g(X)$ is nonlinear and analytically difficult.

present and this makes sampling a spatial field with uniformly distributed sensors impossible.

Let $g(x)$ be a field with bandwidth 2π , which is less than $2b\pi$. Consider the field $g_3(t) = g(mt)$ for any positive integer $m \leq b$. Then $g_3(t)$ is bandlimited with bandwidth up to $2b\pi$. It will be shown that

$$\mathbb{P}(g(U) \leq \theta) = \mathbb{P}(g_3(U) \leq \theta) \quad (8)$$

for any $\theta \in [-1, 1]$ and any $1 \leq m \leq b$. The core idea behind the proof is the accounting of the length of level set. Let

$$\{u : g(u) \leq \theta\} = [x_0, x_1] \cup \dots \cup [x_{N-1}, x_N] \cup \{x_{N+1}, \dots, x_M\} \quad (9)$$

where x_0, x_1, \dots, x_M depend on $g(u)$ and θ . Then, for $m = 2$,

$$\{u : g_3(u) \leq \theta\} \quad (10)$$

$$= \{u : g(2u) \leq \theta\} \quad (11)$$

$$= \left[\frac{x_0}{2}, \frac{x_1}{2} \right] \cup \dots \cup \left[\frac{x_{N-1}}{2}, \frac{x_N}{2} \right] \cup \left[\frac{x_0+1}{2}, \frac{x_1+1}{2} \right] \cup \dots \cup \left[\frac{x_{N-1}+1}{2}, \frac{x_N+1}{2} \right] \cup \left\{ \frac{x_{N+1}}{2}, \dots, \frac{x_M}{2}, \frac{x_{N+1}+1}{2}, \dots, \frac{x_M+1}{2} \right\}. \quad (12)$$

Observe that the lengths of the level sets in (9) and (12) are equal to

$$(x_1 - x_0) + (x_3 - x_2) + \dots + (x_N - x_{N-1}) \quad (13)$$

with the note that single points x_{N+1}, \dots, x_{N+M} in the level sets are zero in length (measure). This observation is true for any $g(x)$ with 3 Fourier series coefficients, and any $x \in [-1, 1]$. So $g(x)$ and $g(2x)$ have the same length of level sets and consequently same distribution $\mathbb{P}(g(U) \leq \theta)$. This result can be also shown in a similar manner for $m = 3, \dots, b$. Thus, even if $n \rightarrow \infty$, the field $g(x)$ cannot be inferred uniquely from $F_{g,n}(\theta)$ which converges to $\mathbb{P}(g(U) \leq \theta)$, $\theta \in [-1, 1]$. This result strengthens our claim that an *alternate distribution* is needed on the unknown sampling locations.

D. Sanov's theorem and hypothesis testing limits

It is natural to use likelihood ratio test in a detection setup. To analyze the detection error-probability, large deviation analysis setup will be used. Sanov's theorem, which addresses the asymptotic likelihood properties with respect to an incorrect probability model, will be used [15, Chap 11.4]. Let R_1, \dots, R_n be i.i.d. random variables with discrete distribution \vec{p} . Then, the observed distribution of R_1, \dots, R_n lies in the closed set E with the following probability

$$\lim_{n \rightarrow \infty} \frac{1}{n} \log_2 [\mathbb{P}(R_1^n \in E)] = -D(\vec{q}^* \parallel \vec{p}) \quad (14)$$

where $\vec{q}^* = \arg \min_{\vec{q} \in E} D(\vec{q} \parallel \vec{p})$ is the distribution in E that is the closest to \vec{p} in the Kullback Leibler divergence or relative entropy terms. In other words as n becomes large

$$\mathbb{P}(R_1^n \in E) \propto 2^{-nD(\vec{q}^* \parallel \vec{p})}. \quad (15)$$

The quantity $D(\vec{q}^* \parallel \vec{p})$ will be termed as the *error-exponent* in this work.

III. FIELD DETECTION AND ITS PERFORMANCE

In this section, our field detection algorithm and its performance is discussed where the samples are not affected by measurement noise. The optimal probability distribution, with which sensors should be deployed at various sampling locations, will be derived to minimize the detection error probability of the underlying spatially bandlimited field in this section.

A. The field detection algorithm

At first, it will be shown that the type of observed field values is a sufficient statistic for detection. Then, a clustering algorithm will be presented that uses the type of observed field values.

Since the field is sampled at $(2b+1)$ distinct locations, the samples Y_1, \dots, Y_n take $(2b+1)$ distinct values as discussed in Section II-A. Let $\vec{V} = [V_0, V_1, \dots, V_{2b}]^T$ denote the vector of these values. It is observed that field values at the sampling locations $g(k s_b), 0 \leq k \leq 2b$ are an unknown permutation of the elements of \vec{V} . There are $(2b+1)!$ distinct permutations of \vec{V} . The goal of our field detection algorithm should be to assign the correct location $k s_b, 0 \leq k \leq 2b$ to each element of \vec{V} . That is, the correct permutation which relates \vec{V} with the true field samples is desired.

Let $\vec{M} = [M_0, \dots, M_{2b}]^T$ denote the vector of types corresponding to the values in \vec{V} (i.e., M_k is the type of value V_k). Each permutation of the values corresponds to a permutation of the types as well. Let ρ be a permutation, and let $(\vec{V}^\rho, \vec{M}^\rho)$ be the permuted versions of the value and type vectors, respectively. The goal of detection is to identify the correct permutation ρ^* that leads to the correct assignment of values to the locations.

The field is sampled according to a distribution \vec{p} as defined in Section II-B. Since $g(k s_b), 0 \leq k \leq 2b$ are a permutation of \vec{V} , so the probability distribution of observations Y_1, \dots, Y_n is given by

$$f(\vec{Y}|\rho) = \prod_{k=0}^{2b} p_k^{M_k^\rho}. \quad (16)$$

This satisfies the Fisher-Neyman factorization theorem for sufficient statistic [16] and \vec{M} is the sufficient statistic for our problem.

Based on the readings $g(X_1), g(X_2), \dots, g(X_n)$, the field $g(x)$ has to be detected. The correct detection of the field corresponds to the correct association of recorded field values with their respective locations. From (5) and Section II-A, $\{g(i s_b), p_i\}$ pairs are distinct in both the elements. Each sensor gets deployed at $X = i s_b$, and subsequently records $g(i s_b)$, with probability p_i . The following *clustering algorithm* will be used to ascertain the field samples $g(i s_b)$ that specify the entire field $g(t)$ (see (2)):

- 1) The readings $Y_1 := g(X_1), \dots, Y_n := g(X_n)$, with X_i unknown and in the set $\{0, s_b, \dots, 2b s_b\}$, are collected.
- 2) The values Y_1, Y_2, \dots, Y_n are clustered into (value, type) pairs. Equal values (value) in Y_1, Y_2, \dots, Y_n are grouped together and the number of equal values (type)

is recorded. At most $2b+1$ such pairs exist since $2b+1$ field values are sampled to generate Y_1, \dots, Y_n .

- 3) Empirical probabilities type/n for each value are calculated. For large n , by weak law of large numbers, the empirical probability type/n of each value will be “near” the correct p_i in \vec{p} .
- 4) The value with smallest empirical probability is assigned to $g(0)$, the value with next smallest empirical probability is assigned to $g(s_b)$, and so on till $g(2b s_b)$.

The clustering algorithm above, with a correct and an incorrect detection of the field, is illustrated by an example below.

Example 3.1 (Detection of field with location unaware sensors on a gr)

Consider a signal $g_1(t)$ with bandwidth parameter $b = 1$, and $s_b = \frac{1}{2b+1} = \frac{1}{3}$. The correct field samples at $0, s_b, 2s_b$ are $g_1(0) = 1.06, g_1(1/3) = 1.80, g_1(2/3) = 0.14$.

The field is sampled using $n = 10$ randomly realized values of sensor's location in the set $\{0, 1/3, 2/3\}$. In one realization of this statistical experiment, the 10 observed samples are 1.80, 0.14, 0.14, 1.06, 1.80, 0.14, 1.80, 1.06, 0.14, 0.14. The (value, type) pairs are (1.06, 2), (1.80, 3), and (0.14, 5). The above clustering algorithm concludes that $g_1(0) = 1.06, g_1(1/3) = 1.80, g_1(2/3) = 0.14$, and it correctly associates the field values to the sample locations in this case.

In another realization of the same statistical experiment, the 10 observed samples are 1.06, 0.14, 0.14, 1.06, 1.80, 0.14, 1.80, 1.06, 0.14, 0.14. The (value, type) pairs are (1.06, 3), (1.80, 2), and (0.14, 5). The above clustering algorithm concludes that $g_1(0) = 1.80, g_1(1/3) = 1.06, g_1(2/3) = 0.14$, and it incorrectly associated the field values to the sample locations in this case. ♣

Next, the exponent of the detection error probability of the clustering algorithm will be minimized as $n \rightarrow \infty$. For further discussions on the clustering algorithm described above, define

$$N_i := \sum_{j=1}^n \mathbb{1}[Y_j = g(i s_b)] \quad (17)$$

as the type random variable of $g(i s_b)$ in n field observations. Note that $\mathbb{E}(N_i) = n p_i$ for $0 \leq i \leq 2b$. Since $0 < p_0 < p_1 < \dots < p_{2b}$, as $n \rightarrow \infty$ in the above-mentioned clustering algorithm, by the weak law of large numbers it is expected that

$$0 < N_0 < N_1 < \dots < N_{2b} \quad (18)$$

with high-probability. If the statistical event in (18) on type random variables is not true, the above-mentioned clustering algorithm will result in erroneous field detection. The probability of correct detection in (18) will be maximized by choosing the sensor deployment distribution \vec{p} in what follows.

B. Field detection error-probability minimization

The spatial field is detected correctly when the condition in (18) is satisfied. Let e_n be the detection error-probability. The error-exponent, as the number of sensors n gets large, in the detection error-probability e_n will be maximized in this section. Note that,

$$\begin{aligned} e_n &= \mathbb{P}[(0 < N_0 < N_1 < \dots < N_{2b})^c] \\ &= \mathbb{P}[\{N_0 = 0\} \cup \{N_0 \geq N_1\} \cup \dots \cup \{N_{2b-1} \geq N_{2b}\}]. \end{aligned} \quad (19)$$

By applying the union-bound and the subset-inequality ($A \subseteq B$ implies $\mathbb{P}(A) \leq \mathbb{P}(B)$) in the above equation [17], we get

$$e_n \leq (2b+1) \max \left\{ \mathbb{P}(N_0 = 0), \mathbb{P}(N_0 \geq N_1), \dots, \mathbb{P}(N_{2b-1} \geq N_{2b}) \right\} \quad (20)$$

$$\text{and } e_n \geq \max \left\{ \mathbb{P}(N_0 = 0), \mathbb{P}(N_0 \geq N_1), \dots, \mathbb{P}(N_{2b-1} \geq N_{2b}) \right\}. \quad (21)$$

From the above equations, the error-exponent in e_n is maximized if the error exponent of $\max \left\{ \mathbb{P}(N_0 = 0), \mathbb{P}(N_0 \geq N_1), \dots, \mathbb{P}(N_{2b-1} \geq N_{2b}) \right\}$ is maximized. The constant factor $(2b+1)$ in (20) does not contribute to the error-exponent, since it does not depend on n . The error-exponent maximization of the right side in (21) is addressed in the next theorem.

Theorem 3.1: Let $s_b = 1/(2b+1)$ and $p_i = \mathbb{P}(X_i = is_b)$, for $0 \leq i \leq 2b$, the chance that a sensor lands at location is_b . Let $N_i = \frac{1}{n} \sum_{i=0}^n \mathbb{1}(X_i = is_b)$ be the number of sensors at location is_b . Then, for e_n as defined in (19), the error-exponent is minimized when the sensor deployment probabilities are chosen according to the rule

$$p_i^* = \frac{3(i+1)^2}{(b+1)(2b+1)(4b+3)} \text{ for } 0 \leq i \leq 2b. \quad (22)$$

It can be verified that $\sum_{i=0}^{2b} p_i^* = 1$ for this rule.

Proof: This exponent minimizes the detection error probability of the clustering scheme in Section III-A. A sensor falls at location 0 with probability p_0 . With n randomly deployed sensors,

$$\mathbb{P}[N_0 = 0] = (1 - p_0)^n. \quad (23)$$

Unlike the first term $\mathbb{P}[N_0 = 0]$, other events $\mathbb{P}[N_i \geq N_{i+1}], 0 \leq i \leq 2b$ will be difficult to compute exactly since the random variables N_0, N_1, \dots, N_{2b} are dependent. To obtain the error exponents of these terms, Sanov's theorem will be used (see (14)).

The empirical distribution of the cluster types is $\vec{q} = [\frac{N_0}{n}, \frac{N_1}{n}, \dots, \frac{N_{2b}}{n}]$. In accordance with the Sanov's theorem, an empirical distribution \vec{q} will be found such that $D(\vec{q} \| \vec{p})$ is minimum, subject to the condition $N_0 > N_1$. This will result in the error exponent of the event $\mathbb{P}(N_0 > N_1)$ (see (14)). The empirical distribution is $\vec{q} = [\frac{N_0}{n}, \frac{N_1}{n}, \dots, \frac{N_{2b}}{n}]$ and, from Sanov's theorem, the function to be minimized is

$$D(\vec{q} \| \vec{p}) = \sum_{i=0}^{2b} \frac{N_i}{n} \log_2 \frac{N_i}{np_i} \quad \text{subject to } \sum_{i=0}^{2b} \frac{N_i}{n} = 1 \text{ and } N_1 \leq N_0. \quad (24)$$

The cost-function is convex in the variables N_i , and the constraints on N_i are affine; as a result, the optimal solution must satisfy the KKT conditions [18]. The corresponding Lagrangian is

$$L = \sum_{i=0}^{2b} \frac{N_i}{n} \log_2 \frac{N_i}{np_i} + \lambda \left(\sum_{i=0}^{2b} N_i - n \right) + \mu(N_1 - N_0)$$

At the minima of $D(\vec{q} \| \vec{p})$ in (24),

$$\frac{\partial L}{\partial N_i} = 0 \quad \text{for } 0 \leq i \leq 2b \quad (25)$$

The solutions of above equation are

$$N_0 = \frac{np_0}{e} 2^{-n(\lambda-\mu)}, N_1 = \frac{np_1}{e} 2^{-n(\lambda+\mu)}, \quad (26)$$

and,

$$N_i = \frac{np_i}{e} 2^{-n\lambda} \text{ for } i \geq 2. \quad (27)$$

According to the KKT condition for complementary slackness, at the optimal point we must have [18]

$$\mu(N_1 - N_0) = 0, \quad (28)$$

which is possible if and only if $\mu = 0$ or $N_0 = N_1$. If $\mu = 0$ then

$$N_i = \frac{np_i}{e} 2^{-n\lambda} \text{ for all } 0 \leq i \leq 2b. \quad (29)$$

Substituting this in the constraint $\sum_{i=0}^{2b} N_i = n$, we get:

$$\sum_{i=0}^{2b} N_i = \sum_{i=0}^{2b} \frac{np_i}{e} 2^{-n\lambda} = n \quad (30)$$

Since $\sum_{i=0}^{2b} p_i = 1$ this reduces to $\frac{2^{-n\lambda}}{e} = 1$. Thus the solution in this case is $N_i = np_i$. However since we only consider the family of distributions for which $p_0 < p_1 < \dots < p_{2b}$ this violates the constraint $N_1 \leq N_0$ (since $np_1 > np_0$). Hence the optimal solution corresponds to the case $N_1 = N_0$, which gives $\mu = \frac{1}{2n} \log_2 \left(\frac{p_1}{p_0} \right)$.

For finding λ , note that $\sum_{i=0}^{2b} N_i = n$. Using N_0, N_1 from (26) and N_i from (27) results in

$$\lambda = -\frac{1}{n} \log_2 \left(\frac{e}{1 - (\sqrt{p_1} - \sqrt{p_0})^2} \right) \quad (31)$$

This value of λ gives

$$N_i = \frac{np_i}{1 - (\sqrt{p_1} - \sqrt{p_0})^2} \quad \text{and } N_0 = N_1 = \frac{n\sqrt{p_0 p_1}}{1 - (\sqrt{p_1} - \sqrt{p_0})^2}.$$

Substitution of N_0, N_1, \dots, N_{2b} from the above equation in (24) results in the desired minimum value of $D(\vec{q}^* \| \vec{p})$,

$$D(\vec{q}^* \| \vec{p}) = \log_2 \frac{1}{1 - (\sqrt{p_1} - \sqrt{p_0})^2} \quad (32)$$

For $N_i \geq N_{i+1}$, the optimization constraint $N_0 \geq N_1$ will get replaced by $N_i \geq N_{i+1}$ in (24). The analysis is identical and the result is

$$D(\vec{q}^* \| \vec{p}) = \log_2 \frac{1}{1 - (\sqrt{p_{i+1}} - \sqrt{p_i})^2}. \quad (33)$$

Let $d_0 = \sqrt{p_0}$ and $d_i = \sqrt{p_i} - \sqrt{p_{i-1}}$, $1 \leq i \leq 2b$ and let $d_{\min} = \min\{d_0, d_1, \dots, d_{2b}\}$. Then d_{\min} will determine the value of the largest term in $\max \left\{ \mathbb{P}(N_0 = 0), \mathbb{P}(N_0 \geq N_1), \dots, \mathbb{P}(N_{2b-1} \geq N_{2b}) \right\}$. This is by Sanov's theorem which asserts that $\mathbb{P}(N_i \geq N_{i+1}) \propto 2^{-nD(\vec{q}^* \| \vec{p})}$. Consequently, the value of d_{\min} has to be maximized.

Let \vec{p}^* be the probability for which d_{\min} is maximized. Then,

$$(2b+1)d_{\min} \leq \sum_{i=0}^{2b} d_i = \sqrt{p_{2b}}. \quad (34)$$

To satisfy equality in (34),

$$\sqrt{p_0^*} = \frac{\sqrt{p_{2b}^*}}{2b+1} \text{ and } \sqrt{p_{i+1}^*} = \sqrt{p_i^*} + \frac{\sqrt{p_{2b}^*}}{2b+1}. \quad (35)$$

This relationship, along with $p_0^* + \dots + p_{2b}^* = 1$, results in

$$p_i^* = \frac{3(i+1)^2}{(b+1)(2b+1)(4b+3)} \text{ for } 0 \leq i \leq 2b. \quad (36)$$

This law on \vec{p}^* ensures that the field detection error probability in (19) is *minimized*, and is the *main result* of this work. ■

Observe that the probability e_n in (19) will be minimized if $p_0 < p_1 < \dots < p_{2b}$ are spaced as far as possible. However, there is a constraint on the sum of these probabilities. The rule in (36) specifies how should elements of \vec{p}^* be spaced to minimize detection-error probability.

C. Controlling the detection-error probability

The probability law obtained in the previous section has the minimum detection error probability that converges to zero asymptotically. It is of interest, in practical applications where a field is sampled at unknown locations on a discrete grid, to find the number of samples n which guarantees that any field of bandwidth b can be estimated with detection-error probability, e_n , less than some threshold $\epsilon > 0$.

A sufficient condition for $e_n \leq \epsilon$ is

$$(2b+1)(1 - d_{\min}^2)^n \leq \epsilon. \quad (37)$$

Taking logarithm on both sides results in

$$n \log_e(1 - d_{\min}^2) \geq \log_e\left(\frac{\epsilon}{(2b+1)}\right) \quad (38)$$

$$\text{or } n \geq \frac{\log_e(\epsilon) - \log_e(2b+1)}{\log_e(1 - d_{\min}^2)} \quad (39)$$

This is a sufficient condition on the number of samples required to reduce the detection error probability below a specified threshold for a field of given bandwidth.

D. Simulation Results

Using MATLAB, the detection error-probability was compared for different laws on \vec{p} . Fields with bandwidth parameter $b = 3, b = 5, b = 10$, and $b = 20$ were used. The real and imaginary parts of the field's Fourier Series coefficients (for each bandwidth) were selected by i.i.d. samples of a uniform random variable. The number of randomly collected samples for each field was varied between 100 to 10000 for the fields of bandwidth 3, 5, 10, and between 100 to 100000 for the field of bandwidth 20. The empirical detection error-probability, when calculated using 10000 Monte-Carlo trials, is plotted in Fig. 2. A log-log plot is used to understand the detection error probability exponent. Four different \vec{p} were used for comparison and include: (i) the optimal distribution in (36), (ii) a linear distribution $\vec{p} = [\alpha_1, 2\alpha_1, \dots, (2b+1)\alpha_1]$,

(iii) a cubic distribution $\vec{p} = [\alpha_2, 8\alpha_2, \dots, (2b+1)^3\alpha_2]$, and (iv) ordered uniformly distributed random variable realizations based distribution $\vec{p} = \alpha_3[U(1), U(2), \dots, U(2b+1)]$. The constants $\alpha_1, \alpha_2, \alpha_3$ were selected to ensure that $\sum_{i=0}^{2b} p_i = 1$. From the plots, the distribution discovered in (36) results in smallest detection error-probability (as expected) for all bandwidths. The number of samples required to reach zero detection error probability increases with increasing bandwidth and the optimal distribution in (36) is the one whose detection-error probability decays fastest to zero in all the observed cases.

For the optimal distribution we also simulated the number of samples required to reduce the empirical detection error probability P_e to 1% for fields of bandwidth 3, 5, 10, and 20 respectively. The Fourier Series coefficients of each field was picked by a uniform random number generator. A binary search algorithm was used to locate the sample size for $0.01 - 0.001 \leq P_e \leq 0.01 + 0.001$. The tolerance of 0.001 is used since the detection error probability is calculated as the fraction of incorrectly detected samples from Monte Carlo simulations and so it need not be exactly equal to 0.01. The results are plotted in Fig. 3.

IV. RECONSTRUCTION FROM NOISY SAMPLES

In this section, the effect of measurement-noise will be evaluated on the location-unaware sensing scheme analyzed so far. Consider the case where the field is sampled as described in Section II-B and the samples are then affected by zero mean, independent, additive Gaussian noise with a known variance σ^2 . In Section III, the core idea was to cluster the observed samples into $(2b+1)$ type-value pairs. If additive measurement-noise is present, no two samples will be equal with high probability. In that case, type-value pair based field detection technique will have to be leveraged by clustering noise-affected samples. This section explores the clustering of n noise-affected samples into $(2b+1)$ clusters quantitatively.

It is assumed that the distribution with which the sensors are deployed at respective grid-point remains as in (36). Since measurement-noise will affect the field detection process further, it is expected that the probability of error for field detection in the noisy case will be higher. This increase in probability of error in field detection will be characterized in this section. Any noise free sample $g(T_i)$, $1 \leq i \leq n$ has a value equal to $g(j s_b)$ for some $0 \leq j \leq 2b$ as discussed in Section III-A. With zero mean independent Gaussian measurement noise with variance σ^2 , our field detection algorithm is as follows:

- 1) The samples $Y_1 := g(T_1) + W_1, \dots, Y_n := g(T_n) + W_n$, with T_i unknown and in the set $\{0, s_b, \dots, 2bs_b\}$, and $W_1, W_2, \dots, W_n \sim \mathcal{N}(0, \sigma^2)$ are obtained.
- 2) Since $T_i = ks_b$ with probability p_k for all $1 \leq i \leq n$, the readings Y_i follow the following Gaussian mixture model (GMM) distribution:

$$f_Y(y) = \sum_{k=0}^{2b} p_k G(y, g(ks_b), \sigma^2) \quad (40)$$

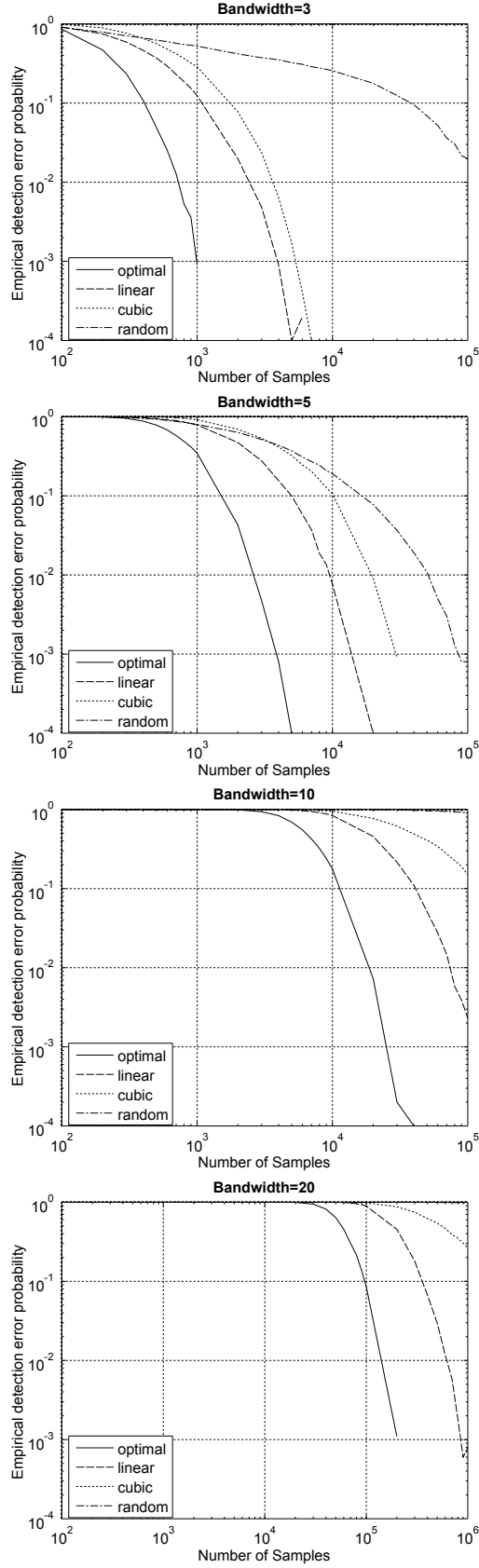


Fig. 2. Detection error-probabilities for different laws on \vec{p} and different bandwidths are compared. The four laws used include the optimal \vec{p} in (36), a linear law, a cubic law, and a randomly generated \vec{p} . Fields of bandwidth 3, 5, 10, and 20 are studied. As expected, the law in (36) is the best in performance in all cases.

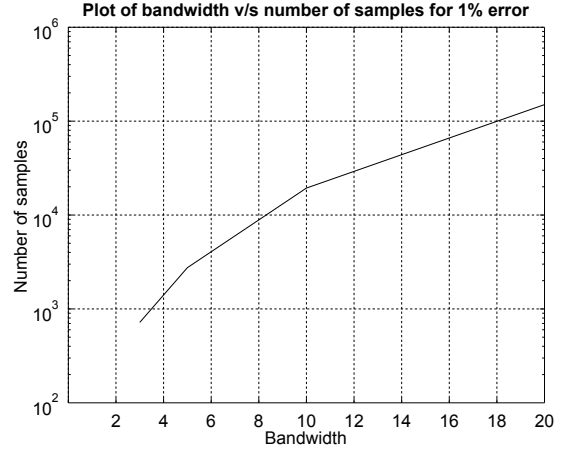


Fig. 3. Number of samples required to reduce the empirical detection error probability to 1% for fields of bandwidth 3, 5, 10, and 20

where

$$G(y, g(k s_b), \sigma^2) = \frac{1}{\sqrt{2\pi}\sigma} \exp\left(-\frac{(y - g(k s_b))^2}{2\sigma^2}\right) \quad (41)$$

- 3) Using the readings Y_1, Y_2, \dots, Y_n , the parameters $(p_k, g(k s_b))$, $k = 0, 1, \dots, 2b$ have to be estimated. To address this estimation problem, the readings Y_1, Y_2, \dots, Y_n are clustered using the well known expectation maximization (EM) algorithm [19], for GMM parameter estimation.
- 4) The algorithm gives an estimate of the *weights* p_k and *means* $g(k s_b)$ (analogous to *type* and *value* in the noiseless case. In the setup, the value of σ is assumed to be known. Let \hat{p}_k and $\hat{g}(k s_b)$ be the estimated *weights* and the corresponding *means*, respectively for $0 \leq k \leq 2b$. For large n , the estimated *weight* \hat{p}_k for each *mean* will be near the correct p_k .
- 5) The *mean* $\hat{g}(k s_b)$ with smallest *weight* is estimated as $g(0)$, the *mean* with next smallest *weight* is estimated as $g(s_b)$, and so on till $g(2b s_b)$.

The EM algorithm iteratively estimates the parameters of the GMM by creating a function for the expectation of the log likelihood function using the current estimate of parameters (E-step) and maximizing this expected log-likelihood to compute a new estimate of the parameters (M-step). These two steps are repeated until the algorithm converges to a maximum of the log likelihood function to obtain an estimate of the means and the weights. In this work, EM algorithm for ‘soft’ segmentation of the data is used [20]. The data comprises of the readings Y_1, Y_2, \dots, Y_n which are segmented into clusters. A cluster is defined as the set of all Y_i that are obtained from $g(k s_b)$ for a fixed k . Thus there are $2b + 1$ clusters in this case. Instead of assigning each reading to a single cluster, a membership matrix Γ is created. The (i, k) element in Γ records a value that indicates the membership of Y_i in the k^{th} cluster.

The membership matrix Γ resolves conflicting situations

where the values of any two or more $g(k s_b)$ are very close in Euclidean distance and their corresponding clusters overlap. Samples lying in overlapping clusters could have originated from either of the sampling locations making it difficult to assign them to a single cluster. The algorithm requires an initial guess of the means which is provided using the k -means++ algorithm [21]. The weights, \hat{p}_k are initially assumed to be uniformly distributed. The variance of the clusters is known (σ^2) and is fixed at this value. Each iteration of the algorithm involves the following two steps:

1) The E-Step:

$$\gamma_{ik} := (\Gamma)_{i,k} = \frac{G(Y_i, \hat{g}(k s_b), \sigma^2) \hat{p}_k}{\sum_{k=0}^{2b} G(Y_i, \hat{g}(k s_b), \sigma^2) \hat{p}_k} \quad (42)$$

2) The M-Step:

$$\hat{g}(k s_b) = \sum_{i=0}^n Y_i \gamma_{ik} \text{ and } \hat{p}_k = \frac{\sum_{i=0}^n \gamma_{ik}}{n} \quad (43)$$

The values of $\hat{g}(k s_b)$ and \hat{p}_k estimated in the M-step are substituted in the E-step of the next iteration and the process is repeated until the estimates converge (squared Euclidean distance between the current and previous estimates of $\hat{g}(k s_b)$ falls below a specified threshold).

The final GMM estimated by the EM algorithm is:

$$\hat{f}_Y(y) = \sum_{k=0}^{2b} \hat{p}_k G(y, \hat{g}(k s_b), \sigma^2). \quad (44)$$

The above algorithm was simulated using MATLAB on 10000 randomly generated fields with three values of total number of samples $n = 1000, 10000, 100000$, and where the samples were corrupted by Gaussian noise ($\mu = 0, \sigma = 0.05$). The experiment was repeated for fields with bandwidth parameter $b = 3, b = 5$, and $b = 10$. The following distortion metric was used:

$$D = \frac{\int_0^1 |\hat{g}(t) - g(t)|^2 dt}{\int_0^1 |g(t)|^2 dt} \quad (45)$$

where D is the distortion, $\hat{g}(t)$ is the estimated field, $g(t)$ is the original field and the limits of the integral are so chosen because the field has a period 1. Histograms of the distortion for each of the experiments are shown in Fig. 4, Fig. 5, and Fig. 6.

From the histograms in Fig. 4, Fig. 5, and Fig. 6 the performance of the algorithm deteriorates on increasing the bandwidth b . The number of fields reconstructed with a low value for distortion decreases as the bandwidth changes from $b = 3$ to $b = 10$. More than 50% of the fields are reconstructed with a low value of distortion for bandwidth $b = 3$ while the number reduces to about 18% for bandwidth $b = 5$, and less than 1% for bandwidth $b = 10$. Increasing the number of samples drawn improves the performance of the algorithm slightly especially for the higher bandwidths as illustrated by an increase in the height of the first bar on the histogram for bandwidths $b = 5$ and $b = 10$ on increasing the number of samples from 1000 to 10000.

For fields with a higher value of distortion it is anticipated that this high value is due to a large degree of overlap between the clusters. This is observed in Fig. 7, which is a histogram of the minimum pairwise squared Euclidean distance between the values of the underlying field at the sampling locations, $g(k s_b)$ for the different experiments. These values serve as the true cluster means and as can be seen from the histogram plots, increasing the bandwidth increases the number of cases in which two different clusters' means lie close to each other. The closeness of cluster means is indicated by an increase in the height of the first bar of the histogram and a decrease in the bin width. This closeness of cluster means explains the poor performance of the reconstruction algorithm with increasing bandwidth.

For a Gaussian distribution, $\mathcal{N}(\mu, \sigma^2)$, 99.7% of the data lies within $[\mu - 3\sigma, \mu + 3\sigma]$. Thus if x_1 and x_2 are the means of two normal distributions with the same standard deviation σ , and $x_2 > x_1$ the corresponding clusters of samples drawn overlap with a high probability, if $x_2 - 3\sigma < x_1 + 3\sigma$ or $(x_2 - x_1)^2 < 6\sigma^2$. For $\sigma = 0.05$, $6\sigma^2 = 0.09$. Thus if the squared Euclidean distance between any two cluster centers ($g(k s_b)$) falls below this value then the corresponding clusters overlap with a high probability leading to an incorrect reconstruction. The problem of overlapping clusters is a common problem in clustering especially with the EM algorithm. Several approaches to solving this problem exist in literature (see, e.g., [22], [23]). The application of these approaches to the present problem remains to be studied.

In all our analysis, the distribution of the noise is assumed to be independent and Gaussian. If the distribution of the noise is non-Gaussian, the mixture-model and the clustering algorithm will have to be changed to suit the noise distribution.

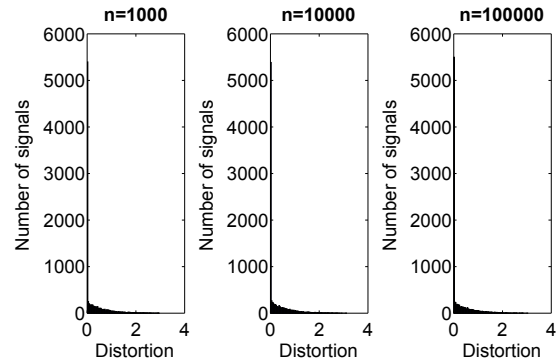


Fig. 4. Results of the sampling and estimation experiment for 10000 randomly generated signals of bandwidth parameter $b = 3$. Histograms of the distortion are plotted for each sample size (n)

V. CONCLUSION

Asymmetric (nonuniform) distributions on location-unaware sensors that enable bandlimited field inference were studied.

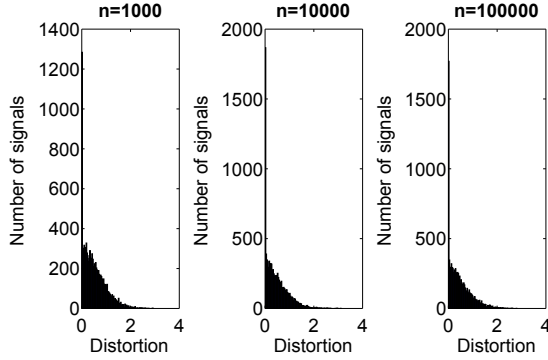


Fig. 5. Results of the sampling and estimation experiment for 10000 randomly generated signals of bandwidth parameter $b = 5$. Histograms of the distortion are plotted for each sample size (n)

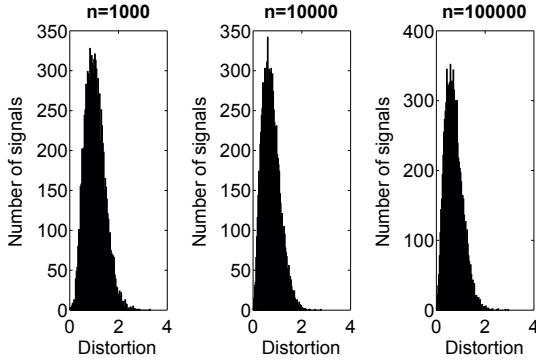


Fig. 6. Results of the sampling and estimation experiment for 10000 randomly generated signals of bandwidth parameter $b = 10$. Histograms of the distortion are plotted for each sample size (n)

For analytical tractability, location-unaware sensors on a *discrete grid* were studied. The key idea was to use associate the samples with their locations by matching the observed type (frequency) and the expected type. Based on this key idea, the main result of this work was to find the *optimal* probability distribution on sensor locations that minimizes the detection error-probability of the underlying spatial field. It was shown that the detection error-probability decreases exponentially fast in the number of sensors deployed. The proposed sampling algorithm was also extended to include the case of field reconstruction in the presence of additive measurement-noise. This was achieved by treating the distribution of the noisy samples as a mixture model and using clustering to estimate the mixture model parameters. Simulations which explored the tradeoffs between the measurement-noise, increase in bandwidth, and the number of samples obtained were showcased.

The cases where sensors are located with an arbitrary continuous distribution in field's support is left for future work.

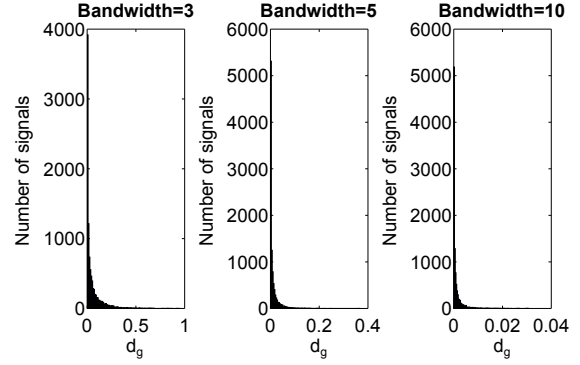


Fig. 7. Minimum pairwise squared Euclidean distance (d_g) between the signal values at the sampling locations, is compared for signals of bandwidth 3, 5 and 10. Histograms of d_g are plotted using 10000 randomly generated signals for each value of bandwidth

REFERENCES

- [1] Animesh Kumar, Prakash Ishwar, and Kannan Ramchandran, "Dithered A/D conversion of smooth non-bandlimited signals," *IEEE Trans. Signal Proc.*, vol. 58, no. 5, pp. 2654–2666, May 2010.
- [2] Animesh Kumar, Prakash Ishwar, and Kannan Ramchandran, "High-resolution distributed sampling of bandlimited fields with low-precision sensors," *IEEE Transactions on Information Theory*, vol. 57, no. 1, pp. 476–492, Jan. 2011.
- [3] J. Murray-Bruce and P. L. Dragotti, "Estimating localized sources of diffusion fields using spatiotemporal sensor measurements," *IEEE Trans. Signal Proc.*, vol. 63, no. 12, pp. 3018–3031, Jun. 2015.
- [4] Jayakrishnan Unnikrishnan and Martin Vetterli, "Sampling and reconstruction of spatial fields using mobile sensors," *IEEE Trans. Signal Proc.*, 2013.
- [5] D. Marco, E. J. Duarte-Melo, M. Liu, and D. L. Neuhoff, "On the many-to-one transport capacity of a dense wireless sensor network and the compressibility of its data," in *IPSN, Proc. of the 2nd Intl. Wkshp., Palo Alto, CA, USA*, LNCS edited by L. J. Guibas and F. Zhao, Springer, NY, 2003, pp. 1–16.
- [6] Juri Raniere and Martin Vetterli, "Sampling and reconstructing diffusion fields in presence of aliasing," in *Proc. of the ICASSP 2013*, 2013.
- [7] Karthik Sharma and Animesh Kumar, "Sampling Smooth Spatio-Temporal Physical Fields: When Will the Aliasing Error Increase With Time?," in *Proc. of the IEEE International Conf. on Acoustic Speech and Signal Processing*, New York, NY, USA, 2015, IEEE.
- [8] Neal Patwari, Joshua N. Ash, Spyros Kyperountas, Alfred O. Hero III, Randolph L. Moses, and Neiyer S. Correal, "Locating the nodes: Cooperative localization in wireless sensor networks," *IEEE Signal Processing Magazine*, vol. 22, no. 4, pp. 54–69, Jul. 2005.
- [9] Henk Wymeersch, Jaime Lien, and Moe Z. Win, "Cooperative localization in wireless networks," *Proceedings of the IEEE*, vol. 97, no. 2, pp. 427–450, 2009.
- [10] Animesh Kumar, "On bandlimited signal reconstruction from the distribution of unknown sampling locations," *IEEE Transactions on Signal Processing*, vol. 63, no. 5, pp. 1259–1267, Mar. 2015.
- [11] Animesh Kumar, "Bandlimited field estimation from samples recorded by a location-unaware mobile sensor," in *IEEE International Symposium on Information Theory*. IEEE, 2016, pp. 1257–1261.
- [12] Pina Marziliano and Martin Vetterli, "Reconstruction of irregularly sampled discrete-time bandlimited signals with unknown sampling locations," *IEEE Transactions on Signal Processing*, vol. 48, no. 12, pp. 3462–3471, Dec. 2000.
- [13] Alessandro Nordio, Carla-Fabiana Chiasserini, and Emanuele Viterbo, "Performance of linear field reconstruction techniques with noise and uncertain sensor locations," *IEEE Transactions on Signal Processing*, vol. 56, no. 8, pp. 3535–3547, Aug. 2008.
- [14] A. V. Oppenheim, R. W. Schaffer, and J. R. Buck, *Discrete-Time Signal Processing*, Prentice Hall, USA, 1999.

- [15] T. M. Cover and J. A. Thomas, *Elements of Information Theory*, John Wiley, New York, NY, USA, 1991.
- [16] Peter J. Bickel and Kjell A. Doksum, *Mathematical Statistics Vol I*, Prentice Hall, Upper Saddle River, NJ, USA, 2001.
- [17] R. Durrett, *Probability: Theory and Examples*, Duxbury Press, Belmont, CA, 2nd edition, 1996.
- [18] Stephen Boyd and Lieven Vandenberghe, *Convex optimization*, Cambridge University Press, 2004.
- [19] Arthur P. Dempster, Nan M. Laird, and Donald B. Rubin, "Maximum likelihood from incomplete data via the em algorithm," *Journal of the Royal Statistical Society. Series B (Methodological)*, pp. 1–38, 1977.
- [20] Alexandra Lauric and Sarah Frisken, "Soft segmentation of CT brain data," Tech. Rep., Tufts University, 2007.
- [21] David Arthur and Sergei Vassilvitskii, "*k*-means++: The advantages of careful seeding," in *Proceedings of the Eighteenth Annual ACM-SIAM Symposium on Discrete Algorithms*. Society for Industrial and Applied Mathematics, 2007, pp. 1027–1035.
- [22] Arindam Banerjee, Chase Krumpelman, Joydeep Ghosh, Sugato Basu, and Raymond Mooney, "Model-based overlapping clustering," in *Proceedings of the Eleventh ACM SIGKDD International Conference on Knowledge Discovery in Data Mining*. ACM, 2005, pp. 532–537.
- [23] Qiang Fu and Arindam Banerjee, "Multiplicative mixture models for overlapping clustering," in *Proceedings of the Eighth IEEE International Conference on Data Mining*. IEEE, 2008, pp. 791–796.